# A New Micromachined Overlay CPW Structure With Low Attenuation Over Wide Impedance Ranges and Its Application to Low-Pass Filters

Hong-Teuk Kim, *Student Member, IEEE,* Sanghwa Jung, Jae-Hyoung Park, Chang-Wook Baek, *Member, IEEE,* Yong-Kweon Kim, *Member, IEEE,* and Youngwoo Kwon, *Member, IEEE*

***Abstract*—In this paper, a new micromachined overlay-coplanar-waveguide (OCPW) structure has been developed and its characteristics are studied in detail as a function of the line parameters. In OCPW, the edges of the center conductors are lifted by micromachining techniques and partially overlapped with the ground plane to facilitate low-impedance lines. The elevated center conductors help to reduce the conductor loss by redistributing the current over a broad area. Comparative experiments on low-loss and lossy substrates also confirm the screening effect from the substrate losses by confining the electric field in the air between the overlapped conductor plates. Compared with the coplanar-waveguide (CPW) lines, the OCPW lines show wider impedance range (25–80 $\Omega$) and lower loss ($<$0.95 dB/cm at 50 GHz). The advantages of OCPW for low-$Z_0$ lines are utilized to realize a high-performance stepped-impedance low-pass filter at $X$-band. The OCPW filter shows distinct advantages over the conventional CPW filter in terms of size, loss, skirt, and stopband characteristics.**

***Index Terms*—Coplanar waveguide, low-pass filter, micromachining technology, transmission line.**

## I. Introduction

CONVENTIONAL coplanar-waveguide (CPW) lines suffer from high conductor losses at high and low characteristic impedance $(Z_0)$ extremes due to narrowing of the center conductor and slot width, respectively [1], [2]. Moreover, very low-$Z_0$ lines are practically impossible to realize in CPW due to the minimum slot size limit imposed by the fabrication process. Therefore, designers are often restricted in their choice of impedance values when designing monolithic-microwave integrated-circuit (MMIC) circuits with CPW.

To reduce the losses of the high-$Z_0$ lines, there have been attempts to elevate the center conductor [3]–[5]. The capacitance of the line is decreased in this way and wider center conductors can be used instead of narrow lines. Recently, micromachining techniques have also been applied to reduce the capacitance of the high-$Z_0$ line by removing the high dielectric material, leaving only a thin membrane that suspends transmission lines [6], [7].

As far as the low-$Z_0$ lines are concerned, a thin-film process has been utilized to realize overlap CPW lines where the signal and ground lines are overlapped, but vertically separated by thin polyimide [8], [9]. The overlap between signal and ground lines makes very low-$Z_0$ lines possible without the slot size constraint. However, this approach requires additional process steps and, more importantly, the lines with a dielectric layer of a few micrometers still suffer from high conductor losses due to high field intensities between the signal and ground plates.

Recently, the authors proposed a new overlay-coplanar-waveguide (OCPW) structure, in which the edges of center conductor are partially elevated and overlapped with ground, to achieve broad $Z_0$ ranges and to reduce the line losses [10]. Micromachining techniques allowed metal overlay without resorting to the thin-film process, leaving air between the plates. It also resulted in a large spacing between the metal plates, which was as much as 15 $\mu$m.

In this paper, the loss characteristics of the OCPW lines are studied in detail for various elevation and overlap values. Field simulations and comparative experiments have been performed to fully characterize the OCPW lines. The screening effect from the substrate losses is also investigated by comparing the OCPW lines fabricated on low-loss quartz and lossy glass substrates. Simulated characteristics of the OCPW lines are described in Section II. The detailed fabrication process of the OCPW lines is presented in Section III, together with the measured results in Section IV. To demonstrate the practical usefulness of the OCPW, an $X$-band 0.5-dB equiripple Chebyshev seven-section stepped-impedance low-pass filter (LPF) has been designed and fabricated using low-$Z_0$ OCPW lines. The filter results are compared with the same filter realized with CPW lines in Section V. It is shown that low-$Z_0$ OCPW lines can be used as lumped capacitors, which help to solve the inherent problems of the LPF using distributed structures, such as low cutoff rates and poor attenuation in the stopband. Compared with the CPW filter, the OCPW filter shows distinct advantages such as small size, low insertion loss, sharp skirt characteristics, and wide stopband.

## II. Simulation

The schematic of an OCPW is shown in Fig. 1 together with the associated parameters. The edges of the center conductor are partially elevated using micromachining techniques and are overlapped with the ground. It can be easily seen from the structure that a low-$Z_0$ line can be implemented without additional process difficulty by increasing the overlap ("O" in Fig. 1) between the center conductor and the ground. High-$Z_0$ lines are

Manuscript received November 3, 2000. This work was supported in part by the Korean Ministry of Science and Technology under the Creative Research Initiative Program.

The authors are with the School of Electrical Engineering, Seoul National University, Seoul 151-742, Korea (e-mail: ykwon@snu.ac.kr).

Publisher Item Identifier S 0018-9480(01)07590-1.

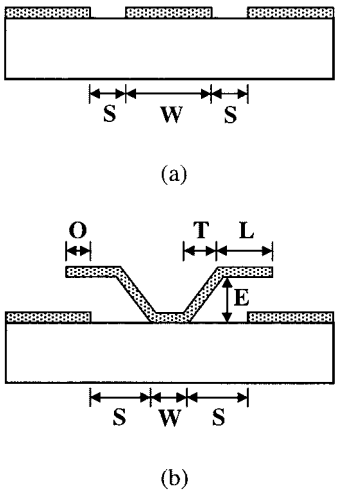


Fig. 1. Schematic diagrams of: (a) CPW and (b) OCPW showing dimension details. Dimensions are specified in the text.

equally easily achievable by employing negative overlap between the two conductors; negative overlap means the separation between the conductors. The OCPW helps to reduce the conductor loss by reducing the field concentration and current crowding at the edges of the signal lines. Moreover, the OCPW is expected to reduce not only the conductor loss, but also the substrate loss by confining the electric field in the air between the overlapped conductor plates.

The loss analysis of both the OCPW ($O = -50, -17, -5, 10, 20, 30, 50$, and $65\ \mu$m) and CPW ($S = 50, 28, 17, 5, 3$, and $2\ \mu$m) lines is performed using a 520-$\mu$m-thick quartz substrate ($\epsilon_r = 3.8, \tan\delta = 0.00033$). The ground-to-ground spacing $(W + 2S)$ is fixed at 200 $\mu$m. In the OCPW, the width of the center conductor touching the substrate is fixed at 30 $\mu$m, and the ascending angle of the sloped length ("$T$" in Fig. 1) is set to 17°. Fig. 2 shows the calculated losses and effective dielectric constants ($\epsilon_{\text{eff}}$'s) as a function of $Z_0$ and elevation $(E)$ for both lines. The simulation is carried out at 50 GHz using a commercial electromagnetic (EM) simulator (IE3D). In case of the CPW lines, it is practically impossible to achieve the $Z_0$ values lower than 30 Ω due to the photolithographical limit that sets the minimum spacing between the signal and ground lines at 2 $\mu$m. On the contrary, a wide impedance range down to 20 Ω can easily be obtained by controlling the overlap (O) in the OCPW. The loss of OCPW lines with a high elevation $(E = 15\ \mu\text{m})$ is maintained to less than 1 dB/cm over a wide impedance range from 20 to 85 Ω, while that of the CPW $(E = 0\ \mu\text{m})$ line increases rapidly as the impedance decreases below 30–40 Ω.

It is also worthwhile to note from Fig. 2(a) that the loss is greatly reduced and become independent of the impedance as the elevation of the signal line increases. OCPW lines with an elevation of 15 $\mu$m shows less than 0.7-dB/cm loss over the entire impedance range from 20 to 85 Ω. On the other hand, the conductor loss improvement is only marginal at a low elevation of 5 $\mu$m. Improved loss reduction at high elevation is attributed to the enhanced spreading of the current over the wide area as the elevation increases. Fig. 2(a) indicates that the elevation should be high enough to have any meaningful impact on the loss and the usable $Z_0$ range. This point proves the advantage

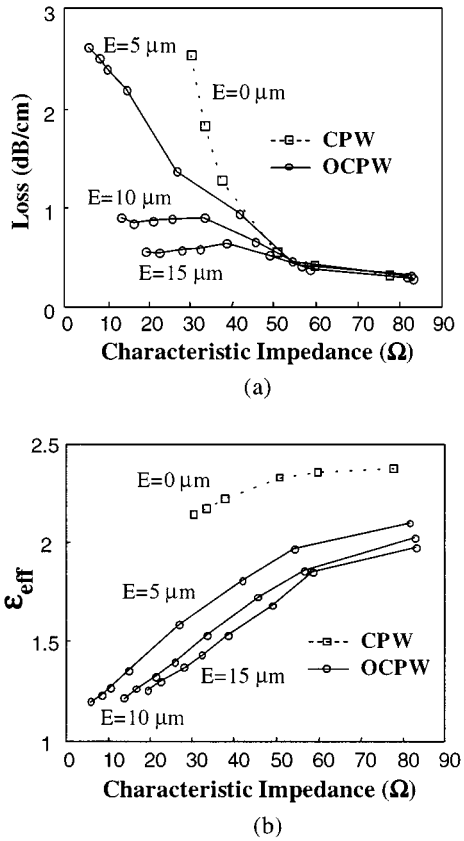


Fig. 2. Comparison of calculated: (a) losses and (b) effective dielectric constants for CPW ($S = 50 \sim 2\ \mu$m) and OCPW ($O = -50 \sim 65\ \mu$m) on a 520-$\mu$m-thick quartz substrate at 50 GHz as a function of $Z_0$ and elevation $(E)$. The ground-to-ground spacing $(W + 2S)$ is fixed to 200 $\mu$m.

of the micromaching techniques over the thin-film technology that permits only limited elevation up to a few micrometers. Fig. 2(b) shows that at a given $Z_0$ value, the effective dielectric constant becomes lower as the elevation increases, which illustrates enhanced field confinement in the air between the overlapped plates at high elevation.

## III. Fabrication

The OCPW lines are fabricated on quartz and glass substrates. The process steps are identical in both cases. All the conductor layers are realized using 3-$\mu$m-thick electroplated gold. The length of each transmission line is 1 cm and the elevation of the signal line is 15 $\mu$m measured from the substrate. Fig. 3 illustrates the fabrication process of the OCPW line. At first, titanium and gold are thermally evaporated on the substrate as a seed layer [see Fig. 3(a)]. The electroplating mold is formed using thick photoresist, through which 3-$\mu$m-thick gold transmission lines are electroplated [see Fig. 3(b)]. The gold electroplating process is carried out using commercially available noncyanide electrolytic solution (NEUTRONEX 210 B) and the electrolytic solution temperature is fixed at 60 °C. The electroplating rate is proportional to current density and electroplating time. The thickness of the electroplated structures can thus be controlled by the electroplating time at the fixed current density. In this study, the current density of the electroplating is fixed at 2 mA/cm$^2$, producing the electroplating rate of 0.125 $\mu\text{m}/\text{min}$. The surface roughness of the electroplated structure is 0.061 $\mu$m. To form a

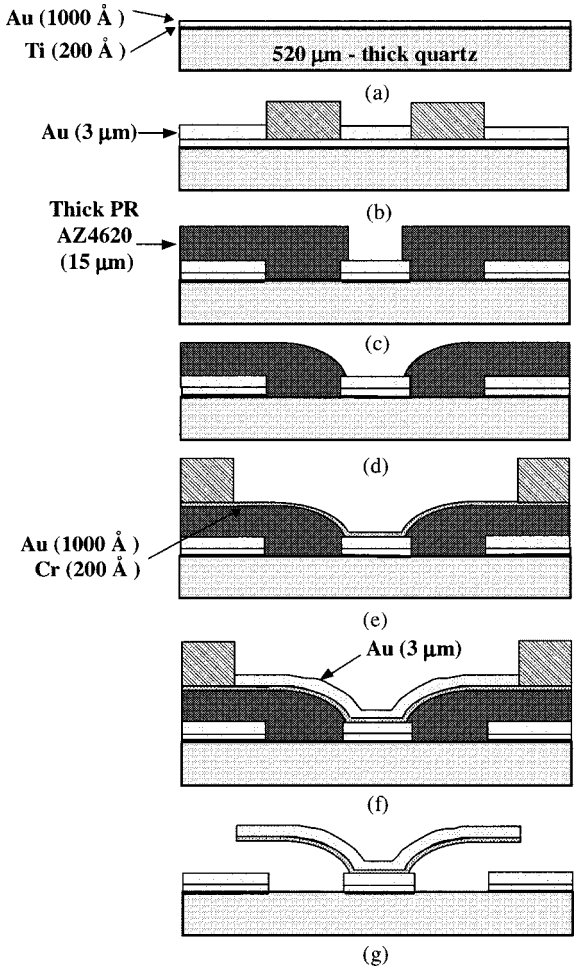


Fig. 3. Fabrication process flow for OCPW line. (a) Seed layer deposition. (b) Photoresist patterning and first metal line electroplating. (c) Sacrificial layer patterning. (d) Sacrificial photoresist curing. (e) Photoresist mold patterning. (f) Second metal line electroplating. (g) Sacrificial layer ashing.

sacrificial layer with a thickness of 15 $\mu$m, a thick photoresist (AZ4620) is spin coated and patterned by UV lithography [see Fig. 3(c)]. The patterned sacrificial layer is thermally cured at a temperature of 200 °C for photoresist reflowing that is required for smooth metal overlay [see Fig. 3(d)]. Next, the seed layer is evaporated and electroplating mold is formed [see Fig. 3(e)]. After electroplating elevated gold structures, the sacrificial layer is ashed with plasma process [see Fig. 3(f) and (g)]). The total ashing time is about 90 min.

## IV. Measurement

Various $Z_0$ OCPW lines are fabricated on both low- and high-loss substrates to demonstrate the effect of the substrate losses. A 520-$\mu$m-thick quartz ($\epsilon_r = 3.8$, $\tan\delta = 0.00033$ at 30 GHz) is used for a low-loss substrate and a 520-$\mu$m-thick glass ($\epsilon_r = 4.6$, $\tan\delta \sim 0.02$ at 50 GHz as extrapolated from the given data sheet) is used for s high-loss substrate. For comparison, CPW lines were also fabricated at the same time on both substrates. The microphotograph of the fabricated OCPW line on the quartz substrate is shown in Fig. 4. The $S$-parameters of the lines were measured by an HP 8510C network analyzer.

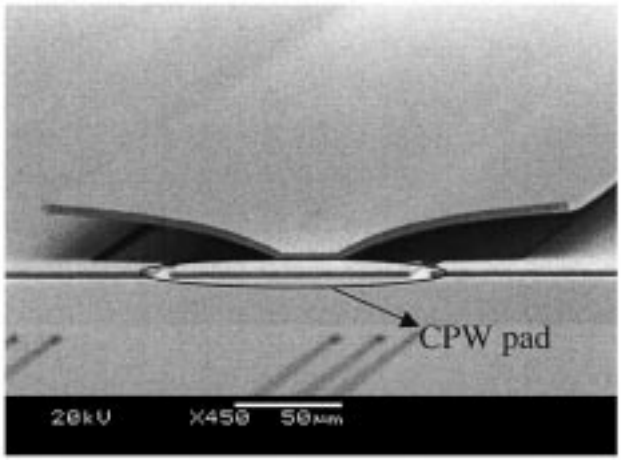


Fig. 4. SEM photograph of the fabricated OCPW line with a CPW-to-OCPW transition for measurement. The wide center conductor represents the probing pad at the CPW end of the integrated CPW-to-OCPW transition.

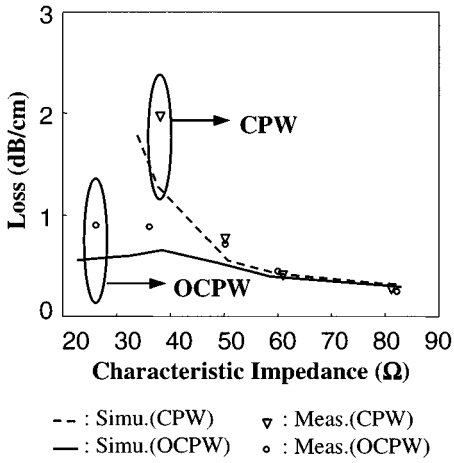


Fig. 5. Measured and simulated losses for CPW ($S = 50, 28, 17,$ and $5$ $\mu$m) and OCPW ($O = -50, -17, -5, 20,$ and $50$ $\mu$m) on a 520-$\mu$m-thick low-loss quartz substrate at 50 GHz as a function of $Z_0$. The ground-to-ground spacing $(W + 2S)$ is fixed to 200 $\mu$m and the elevation $(E)$ is 15 $\mu$m.

First, the measured losses of OCPW ($O = -50, -17, -5, 20,$ and $50$ $\mu$m) and CPW ($S = 50, 28, 17,$ and $5$ $\mu$m) structures on low-loss quartz substrates are compared as a function of $Z_0$ at 50 GHz in Fig. 5. Also shown in Fig. 5 are the simulated loss characteristics for comparison. Lines with five and four different $Z_0$ values are measured for the OCPW and CPW, respectively. At high-$Z_0$ levels (>50 $\Omega$), the OCPW and CPW show comparable losses. However, the losses of the OCPW are maintained to less than 1 dB/cm as the $Z_0$ decreases down to 25 $\Omega$, while those of the conventional CPW increase rapidly at low-$Z_0$ values (2 dB/cm for $Z_0 = 38$ $\Omega$). Fig. 5 clearly shows the advantage of OCPW lines for low-$Z_0$ applications. Due to the negligible dielectric loss of the quartz substrate, the loss is believed to be dominated by the conductor loss arising from current crowding at the conductor edges for CPW lines.

The screening effect from the substrate loss in the OCPW can be demonstrated by comparing the loss characteristics on low-loss quartz and lossy glass substrates. The results on the glass substrates have been reported by Kim *et al.* [10], which included the comparison with the elevated coplanar waveguide

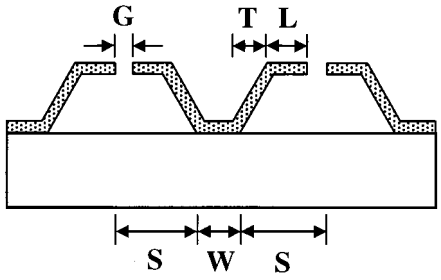


Fig. 6. Schematic diagram of the ECPW line.

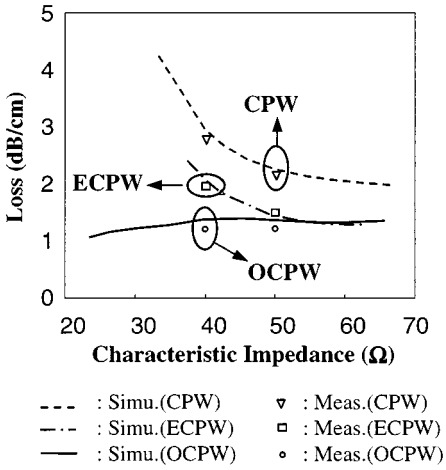


Fig. 7. Measured and simulated losses for CPW ($S = 15,5\ \mu$m), ECPW ($G = 10,4\ \mu$m), and OCPW ($O = -8,10\ \mu$m) structures fabricated on a 520-$\mu$m-thick lossy glass substrate at 50 GHz as a function of $Z_0$. The ground-to-ground spacing $(W + 2S)$ is fixed to 170 $\mu$m and the elevation $(E)$ is 15 $\mu$m.

(ECPW) besides the CPW and OCPW. The schematic of the ECPW is shown in Fig. 6, where the center conductor and ground planes are partially elevated to the same height. Fig. 7 shows the losses of CPW, OCPW, and ECPW structures on the glass substrates as a function of $Z_0$ at 50 GHz [10]. Unlike the case of quartz, OCPW lines show lower losses than the CPW for the entire $Z_0$ range; on quartz, the CPW and OCPW show comparable losses at a high-$Z_0$ range. Lower loss of the OCPW at high-$Z_0$ values is the result of the elevated signal lines, which lessen field penetration into the lossy substrate. This point demonstrates the screening effect from the substrate losses in OCPW lines. Thus, the OCPW can be a good candidate for lossy substrates such as silicon.

The ECPW also shows loss improvement over the CPW. However, the loss increases rapidly at low-$Z_0$ values as in the case of the CPW, which demonstrates that simple elevation of the conductor planes, as in the ECPW, cannot keep the loss from rising at low-$Z_0$ extremes. Loss degradation at low-$Z_0$ values in the ECPW line is caused by a strong electric field at the narrow gap between the ground and signal conductors, as in the case of the conventional CPW structures.

## V. LPF Application

As is well known, stepped-impedance LPFs using distributed structures suffer from low cutoff rates and poor attenuation in

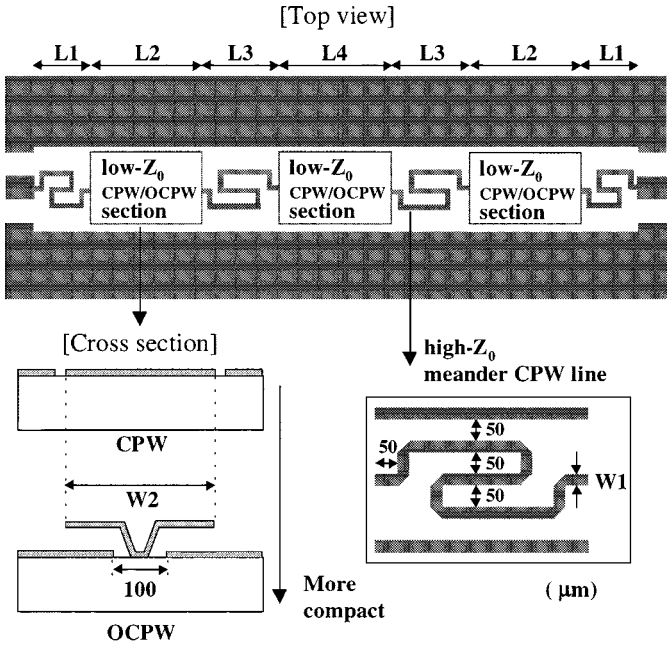


| Filter type (Low $Z_0$) | W1 (μm) | W2 (μm) | L1 (μm) | **L2 (μm)** | L3 (μm) | **L4 (μm)** |
|---|---|---|---|---|---|---|
| CPW | 30 | 290 | 884 | **2766** | 1265 | **2958** |
| OCPW | 30 | 290 | 884 | **1911** | 1265 | **2043** |

Fig. 8. Layouts and detailed dimensions for CPW and OCPW $X$-band LPFs.

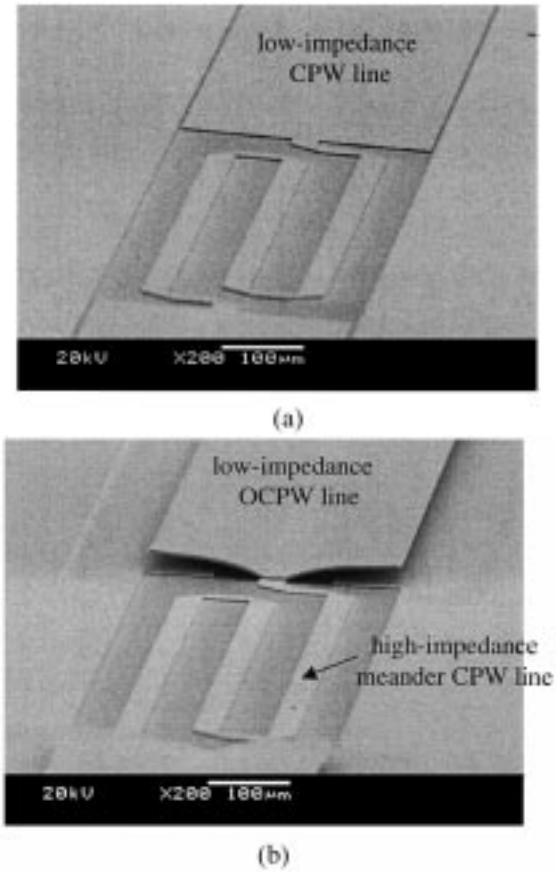


Fig. 9. SEM photographs of single high $Z_0$—low $Z_0$ section used in the $X$-band LPFs. (a) CPW filter. (b) OCPW filter.

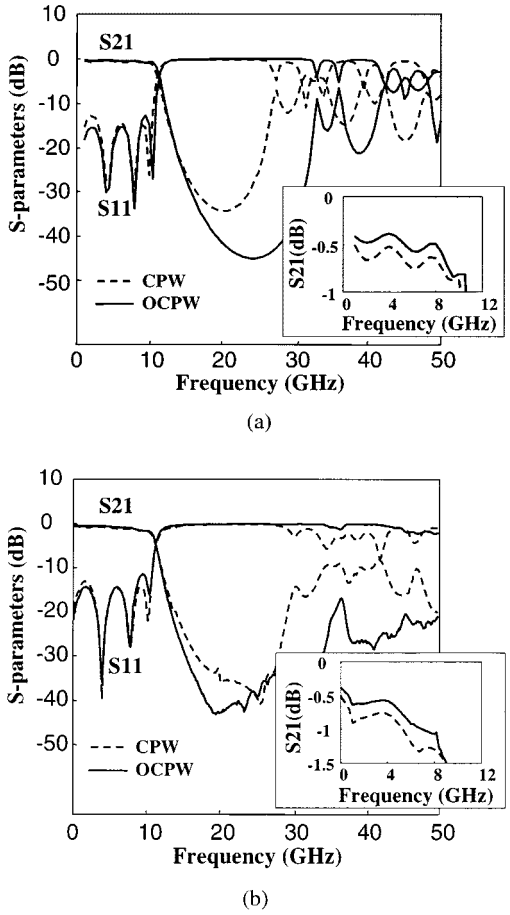


Fig. 10. (a) Simulated and (b) measured responses of both CPW and OCPW $X$-band LPFs.

the stopband [11]. To overcome the limits of conventional filters, numerous research activities have recently been activated in the design of the uniplanar filters, in which lumped capacitors or folded shunt stubs were used as capacitive elements of the filter [12], [13]. In this study, we have employed low-$Z_0$ OCPW lines as capacitive elements in the stepped-impedance LPF. Thus, this LPF is expected to benefit from the low-loss and low-$Z_0$ capabilities of OCPW structures. For experimental verification, $X$-band 0.5-dB equiripple Chebyshev seven-section stepped-impedance LPFs have been implemented using CPW and OCPW lines on 520-$\mu$m-thick quartz.

The element values of the filters were calculated using a standard design procedure [11]. To save the design time, $Z_0$ and $\epsilon_{\text{eff}}$ of each section were first calculated using a commercial EM simulator (IE3D). Based these information, the lengths of each section were determined so that they might meet the element values of the filters. The total response of the filter was finally simulated by cascading the $S$-parameters of each section. In the actual layout, the inductive sections were realized using meandered high-$Z_0$ CPW lines for size reduction and were common to both filters. The capacitive sections were implemented with low-$Z_0$ OCPW lines for the OCPW filter, while low-$Z_0$ CPW lines were employed for the conventional CPW filter. The detailed dimensions and the schematics are shown in Fig. 8.

All the line elements were realized with a fixed ground-to-ground spacing of 300 $\mu$m. The inductance of the high-$Z_0$ line $(W = 30\ \mu\text{m})$ was calculated to be 0.64 nH/mm. The width of the center conductor $(W2)$ of low-$Z_0$ lines was fixed at 290 $\mu$m for both filter cases. Thanks to the enhanced capacitance, the OCPW line showed lower $Z_0$ (18.7 versus 35.2 $\Omega$) together with smaller $\epsilon_{\text{eff}}$ (1.3 versus 2.2) than the CPW line. Therefore, the length of low-$Z_0$ lines of the OCPW filter was reduced to 69% of those of the CPW filter according to Richard's transformation [11]. In this way, the capacitive sections using the low-$Z_0$ OCPW line show the properties more similar to the lumped elements.

The close-up photographs of the fabricated $X$-band CPW and OCPW LPFs with meandered high-$Z_0$ CPW lines are shown in Fig. 9(a) and (b), respectively. The comparison between the simulated and measured performance of both filters is shown in Fig. 10(a) and (b). Good agreement is found between the simulation and measurement. Besides the size reduction effect stated earlier, the OCPW filter offers additional advantages of low insertion loss, sharp skirt, and wide stopband characteristics; an insertion-loss improvement of 0.2 dB is observed at the center of the passband (6 GHz) and high rejection (>20 dB) is obtained over multiple-octave bandwidths (15–50 GHz) in the OCPW LPF.

## VI. Conclusions

In this study, a micromachined OCPW structure was developed to solve the loss problems of the low-impedance CPW lines and to extend the usable impedance ranges. Micromachining was employed to elevate the center conductor and partially overlap it with the ground planes. A systematic and comparative study has been performed to characterize the OCPW lines. It was found that the elevation of the OCPW should be high enough to have meaningful impact on the loss reduction. The experiments on both low-loss quartz and lossy glass substrates show that the OCPW also has a screening effect from the substrate losses. Compared with the conventional CPW, the fabricated OCPW lines with 15-$\mu$m elevation showed lower losses (<0.95 dB/cm on quartz at 50 GHz) over a wider $Z_0$ range (25–80 $\Omega$). To demonstrate practical usefulness of the OCPW lines, an $X$-band stepped-impedance LPF was fabricated using OCPW lines. The OCPW LPF showed distinct advantages over the conventional CPW filter such as lower loss and reduced size, together with improved spurious responses, including sharp skirt and wide stopband characteristics. Thanks to their wide impedance and low-loss characteristics, the proposed OCPW using microelectromechanical system (MEMS) technology is expected to be very useful for various uniplanar microwave/millimeter-wave integrated circuits.

## References

[1] R. W. Jackson, "Considerations in the use of coplanar waveguide for millimeter-wave integrated circuits," *IEEE Trans. Microwave Theory and Tech.*, vol. MTT-34, pp. 1450–1456, Dec. 1986.

[2] K. C. Gupta, R. Garg, I. Bahl, and P. Bhartia, *Microstrip Lines and Slotlines*. Norwood, MA: Artech House, 1996, ch. 7.

[3] M. S. Shakouri, A. Black, B. A. Auld, and D. M. Bloom, "500 GHz GaAs MMIC sampling wafer probe," *Electron. Lett.*, vol. 29, no. 6, pp. 557–558, Mar. 1993.

[4] U. Bhattacharya, S. T. Allen, and M. J. W. Rodwell, "DC–725 GHz sampling circuits and subpicosecond nonlinear transmission lines using elevated coplanar waveguide," *IEEE Microwave Guided Wave Lett.*, vol. 5, pp. 50–52, Feb. 1995.
[5] A. Reichelt and I. Wolff, "New coplanar-like transmission lines for application in monolithic integrated millimeter-wave and submillimeter-wave circuits," in *IEEE MTT-S Int. Microwave Symp. Dig.*, June 1998, pp. 99–102.
[6] N. I. Dib, W. P. Harokopus, Jr., L. P. B. Katehi, C. C. Ling, and G. M. Rebeiz, "Study of a novel planar transmission line," in *IEEE MTT-S Int. Microwave Symp. Dig.*, June 1991, pp. 623–626.
[7] T. M. Weller, L. P. B. Katehi, and G. M. Rebeiz, "High performance microshield line components," *IEEE Trans. Microwave Theory Tech.*, vol. 43, pp. 534–543, Mar. 1995.
[8] T. Tokumitsu, T. Hiraoka, and H. Nakamoto, "Multilayer MMIC using a 3 $\mu$m $\times$ 3-layer dieletric film structure," in *IEEE MTT-S Int. Microwave Symp. Dig.*, June 1990, pp. 831–834.
[9] M. Gillick and I. D. Robertson, "Ultra low impedance CPW transmission lines for multilayer MMIC's," in *IEEE MTT-S Int. Microwave Symp. Dig.*, June 1993, pp. 145–148.
[10] H. T. Kim, S. Jung, J. H. Park, C. W. Baek, Y. K. Kim, and Y. Kwon, "A new micromachined overlap CPW structure with low attenuation over wide impedance ranges," in *IEEE MTT-S Int. Microwave Symp. Dig.*, June 2000, pp. 299–302.
[11] G. Matthaei, L. Young, and E. Jones, *Microwave filters, Impedance Matching Networks, and Coupling Structures*. Norwood, MA : Artech House, 1980.
[12] M. Weller, K. J. Herrick, and L. P. B. Katehi, "Quasi-static design technique for mm-wave micromachined filters with lumped elements and series stubs," *IEEE Trans. Microwave Theory Tech.*, vol. 45, pp. 931–937, June 1997.
[13] K. Hettak, N. Dib, A. Omar, G. Deliies, M. Stubbs, and S. Toutain, "A useful new class of miniature CPW shunt stubs and its impact on millimeter-wave integrated circuits," *IEEE Trans. Microwave Theory Tech.*, vol. 47, pp. 2340–2349, Dec. 1999.

**Hong-Teuk Kim** (S'99) was born in Pusan, Korea, in 1968. He received the B.S. degree from Pusan National University, Pusan, Korea, in 1991, the M.S. degree in electrical engineering from the Korea Advanced Institute of Science and Technology (KAIST), Taejon, Korea, in 1993, and is currently working toward the Ph.D. degree at the Seoul National University, Seoul, Korea.

From 1993 to 1998, he was with the LG Central Institute of Technology (LGCIT), where he was engaged in low-noise system integration and superconductor RF filter design for wireless application. His current research is focused on MMIC design, RF MEMS design, and analysis of oscillator phase noise.

**Sanghwa Jung** was born in Korea, in 1973. He received the B.S. degree in electrical engineering from the Seoul National University, Seoul, Korea, in 1999, and is currently working toward the M.S. degree at the Seoul National University.

His current research activities include the design of MMICs for microwave and millimeter-wave systems and application of micromachining techniques to millimeter-wave systems.

**Jae-Hyoung Park** received the B.S. and M.S. degrees in electrical engineering from the Seoul National University, Seoul, Korea, in 1997 and 1999, respectively, and is currently working toward the Ph.D. degree in electrical engineering at the Seoul National University.

He is currently with the Electroplating Micromachining Group, Micro Sensors and Actuators (MiSA) Laboratory, Seoul National University. From 1997 to 1998, his main research activities were the manipulation of microparticles. Since 1998, his research has concerned the design and fabrication of RF MEMS devices.

**Chang-Wook Baek** (S'94–M'95) was born in Korea, in 1970. He received the B.S., M.S., and Ph.D. degrees in electrical engineering from the Seoul National University, Seoul, Korea, in 1993, 1995, and 2000, respectively.

He is currently a Post-Doctoral Researcher with the Inter-University Semiconductor Research Center (ISRC), Seoul National University. He is also a Member of Research Staff for the development of micromachined millimeter-wave device with the Center for 3-D Millimeter-Wave Integrated Systems, Seoul National University. His current research interests are mainly focused on MEMS, including silicon and electroplating microfabrication, material characterization techniques, and RF/millimeter-wave MEMS devices.

**Yong-Kweon Kim** (S'90–M'90) received the B.S. and M.S. degrees in electrical engineering from the Seoul National University, Seoul, Korea, in 1983 and 1985, respectively, and the Dr. Eng. degree from the University of Tokyo, Tokyo, Japan, in 1990. His doctoral dissertation concerned modeling, design, fabrication, and testing of microlinear actuators in magnetic levitation using high critical temperature superconductors.

In 1990, he joined the Central Research Laboratory, Hitachi Ltd., Tokyo, Japan, where he was a Researcher involved with actuators of hard disk drives. In 1992, he joined the Seoul National University, where he is currently an Associate Professor of electrical engineering. His current research interests are modeling, design, and fabrication and testing of electric machines, especially MEMS, microsensors, and actuators.

**Youngwoo Kwon** (S'90-M'94) was born in Korea, in 1965. He received the B.S. degree in electronics engineering from the Seoul National University, Seoul, Korea, in 1988, and the M.S. and Ph.D. degrees in electrical engineering from The University of Michigan at Ann Arbor, in 1990 and 1994, respectively.

From 1994 to 1996, he was with Rockwell Science Center, where he was involved in the development of various millimeter-wave monolithic integrated circuits based on high electron-mobility transistors (HEMTs) and heterojunction bipolar transistors (HBTs). In 1996, he joined the faculty of the School of Electrical Engineering, Seoul National University. His current research activities include the design of MMICs for mobile communication and millimeter-wave systems, large-signal modeling of microwave transistors, application of micromachining techniques to millimeter-wave systems, nonlinear noise analysis of MMICs, and millimeter-wave power combining.